BLOCK OF SODIUM CONDUCTANCE AND GATING CURRENT IN SQUID GIANT AXONS POISONED WITH QUATERNARY STRYCHNINE

M. D. CAHALAN AND W. ALMERS, *Department of Physiology, University of California, Irvine, Irvine, California 92717, Department of Physiology and Biophysics, University of Washington, Seattle, Washington 98195, and the Marine Biological Laboratory, Woods Hole, Massachusetts 02543 U.S.A.*

ABSTRACT Quaternary strychnine blocks sodium channels from the axoplasmic side, probably by insertion into the inner channel mouth. Block is strongly voltage dependent, being more pronounced in depolarized than in resting axons. Using potential steps as a means to modulate the level of block, we investigate strychnine effects on sodium and gating currents at +50 and −70 mV. We analyze our data in terms of the simplest possible model, wherein only an open channel may receive and retain a strychnine molecule. Our main findings are (*a*) block by strychnine and inactivation resemble each other and (*b*) block of sodium and gating currents by strychnine happen with closely similar time-courses. Our data support the hypothesis of Armstrong and Bezanilla (1977) wherein an endogenous blocking particle causes inactivation by inserting itself into the inner mouth of the sodium channel. Quaternary strychnine may act as an artificial substitute for the hypothetical endogenous blocking particle. Further, we suggest that at least 90% of the rapid asymmetrical displacement current in squid axons is sodium channel gating current, inasmuch as quaternary strychnine can block 90% of the displacement current simultaneously with sodium current.

INTRODUCTION

This second paper in a series of three (Cahalan and Almers, 1979*a*)[1] deals with the effects on sodium and gating currents of a permanently charged analogue of strychnine, *N*-methylstrychnine (NMS). Previous work by Shapiro (1977*a*) on myelinated nerve and by Cahalan and Shapiro (1976) on squid axons has shown that NMS blocks sodium channels from the axoplasmic side, and that block by tertiary strychnine is antagonized by external sodium. If this antagonism also applies to the quaternary NMS, it can be suggested with some certainty that the blocking site lies inside the channel. Besides QX-314 (Cahalan and Almers, 1979*a*), NMS may thus be another compound that blocks sodium channels by insertion into the pore.

Armstrong and Bezanilla (1977) have recently suggested that in the course of normal sodium channel inactivation an endogenous blocking or inactivating particle inserts itself into the channel from the axoplasmic side, stopping ion flow as well as hindering subsequent conformational changes. The second effect appears as a partial and reversible block of gating currents, called "charge immobilization." We find that as NMS blocks open channels, it causes a severe block of gating current indicative of almost complete charge immobilization.

[1]Cahalan, M. D., and W. Almers. 1979. Aftereffects of depolarization in squid giant axons poisoned with quaternary strychnine. Submitted for publication.

In pronase-treated axons, inactivation (Armstrong et al., 1973) and charge immobilization (Armstrong and Bezanilla, 1977) are lost, but NMS reintroduces a time- and voltage-dependent block of sodium current superficially resembling inactivation (Cahalan, 1978) and reintroduces charge immobilization, as we demonstrate here. We may thus have found an artificial substitute for Armstrong and Bezanilla's endogenous blocking particle.

METHODS

The experiments described here were done in June–September, 1976, at the Marine Biological Laboratory, Woods Hole, Mass., on giant axons of the squid *Loligo pealii*. All methods of preparation, data acquisition, and analysis were the same as in Cahalan and Almers (1979*a*), and the reader may consult Table I and Methods of that paper for composition and nomenclature of solutions used. In gating current measurements, each sweep was repeated 5–10 times for signal averaging with 0.1-s interval between each sweep. In some experiments, the sodium inactivation described by Hodgkin and Huxley (1952) was eliminated by following the papain treatment with perfusion with a standard internal saline containing 1 mg/ml pronase CB (Calbiochem-Behring Corp., San Diego, Calif.) besides K^+-glutamate and other electrolytes. Keeping the axon at 12°C resulted in total loss of inactivation within 10 min after adding pronase. The enzyme was then quickly washed out to prevent complete deterioration of the axon, and the experiment began in one of the solutions of Table I of Cahalan and Almers (1979*a*). As before, *x//y* in the figure legend means external solution *x* and internal solution *y*.

All experiments were done with a quaternary analogue of strychnine, NMS. The compound was prepared by Dr. Bert Shapiro (Shapiro, 1977*b*) who kindly provided a sample for these experiments. Unlike the parent compound, strychnine, NMS is membrane impermeant (Shapiro, 1977*b*), but the effects of the two compounds on sodium channels of squid axons are indistinguishable as long as perfusion flow is maintained (Cahalan and Shapiro, 1976). With NMS we expect only one active form (namely the charged one) and only one mode of access to the receptor (Hille, 1977*a*,*b*). Because the drug is membrane impermeant, it could be applied internally without fear of escape from the axoplasm.

RESULTS

Block of Sodium Currents by NMS

Fig. 1 shows membrane currents during step depolarization from −70 to 50 mV with and without internal NMS (1 mM). Results from two axons at two different temperatures are included. Each trace shows an initial small transient of outward gating current that is

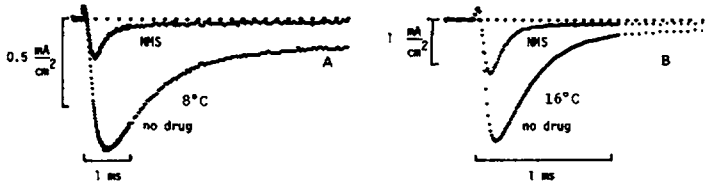

FIGURE 1 Sodium current during depolarization from −70 to +50 mV in two axons at different temperatures before and after internal application of 1 mM NMS. B, axon 198, 16°C; A, axon 81, 8°C. Solutions were Na^+-ASW//200 Cs in both panels. The complete history of axon 81 follows. After preliminary measurements without drug, tetrodotoxin (0.5 μM) was applied at t = 10 min after cannulation. 1 mM internal NMS was added at t = 29 min, and withdrawn at t = 43 min. The gating current measurements of Fig. 4 and 6 (A) were obtained during that period. Tetrodotoxin was washed out at t = 56 min, and the records shown were obtained at t = 96–100 min, ≃ ¼ h after washout of tetrodotoxin. NMS was reapplied at t = 96 min. The experiments of Figs. 1, 2, and 9 were done from t = 90–120 min after cannulation.

followed and partially obscured by a much larger inward sodium current. No potassium outward current is seen in this and all the following experiments because the virtually impermeant Cs^+ replaces all internal K^+. Fig. 1 shows the first major effect of the drug: (*a*) NMS speeds the decline of sodium current during depolarization. In the control, the decline proceeded with final time constants of 1 (Fig. 1 A) or 0.3 ms (Fig. 1 B), reflecting normal, though incomplete, inactivation; in NMS, these values were reduced to 0.3 ms (Fig. 1 A) and 0.14 ms (Fig. 1 B). The effect probably does not reflect a speeding of the normal inactivation process, since NMS actually protects against normal inactivation (see below) and a NMS-induced decline of sodium current remains even after complete removal of inactivation by mild internal digestion with pronase (Cahalan, 1978). Most likely, the abnormally rapid decline of inward current reflects entry of NMS into open channels (Shapiro, 1977*a*), which here evidently happens faster than inactivation.

Fig. 2 shows superimposed records of membrane current during and after depolarizing pulses to 50 mV of varying durations, obtained from the same axons as Fig. 1. Both panels show two further major effects of NMS described and interpreted below.

(*b*) Whereas normally, repolarization is accompanied by a sodium current "tail" characterized by an abrupt increase in inward current followed by rapid decline (top), the tail transients in NMS show a gradual rise ("hook") and decline more slowly. The gradual rise is thought to reflect departure of drug from the channels, as the negative internal potential pulls NMS-cations back into the axoplasm (Shapiro, 1977*a*). The slowing of subsequent decline is expected if Na^+ channels cannot close easily while occupied by NMS. Then even though each drug-free channel may close at its normal rate, the number of open channels remains "buffered" for a while as, with more and more channels becoming unblocked, closing channels continue to be replaced by freshly liberated open channels. Furthermore, traces with and without drug in Fig. 1 superimpose precisely during the first 100–200 μs of the pulse,

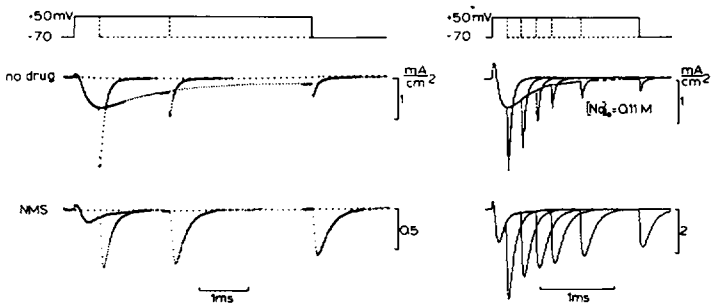

FIGURE 2 Sodium currents during and after depolarizing pulses of varying duration, as indicated schematically (top). Middle traces before, bottom traces after internal application of 1 mM NMS. Records on the left (8°C) from axon 81, all experimental details as in Fig. 1. Records on the right from axon 198 and at elevated temperature (16°C). In the absence of drug, the increase in current upon repolarization appears less abrupt on the right than on the left, because an *x-y* plotter, rather than an oscilloscope, was used to draw the traces on the right. In axon 198, $[Na]_o$ was reduced fourfold when no drug was present to diminish the voltage drop across a possibly incompletely compensated series resistance. In the presence of drug, a 20-s rest period was allowed before each pulse, because depolarization produces, besides the rapid effects described here, a long-lived component of block from which the axon recovers with time constants of the order of 6 s (Cahalan, 1978). Internal solution 200 Cs, external 0.11 M or 0.44 M Na^+-artificial sea water (ASW).

indicating that block occurs after a delay. This is expected if a channel must open before it can be blocked by NMS. These and other findings to be described later support the view that drug-occupied Na^+ channels cannot close easily at -70 mV.

(*c*) Normally, the decline of current during a depolarization follows the same time-course as the decline of tail amplitudes, both being expressions of sodium channel inactivation. In Fig. 2 (top), current during and tail amplitudes after the pulse both diminish in parallel as pulse duration increases. After adding NMS, however, current during the depolarization declines rapidly and almost completely but repolarization is always accompanied by a large tail, even after the longest pulse. After a 5-ms depolarization (left), tail current is actually larger than in the control. In that sense, *NMS* appears to protect against inactivation. A more detailed discussion of this effect is given in a later paper.[1]

Effects *a* and *b* are strongly reminiscent of Armstrong's (1969, 1971) observations on K^+ channels in the presence of certain quaternary ammonium compounds. Extending Armstrong's model, we can view all three kinetic effects of NMS as a consequence of one simple fact: NMS can bind only to open channels. Positive internal potentials drive NMS into the channel; negative potentials pull them back into the perfusate. But before a channel can become blocked by NMS, it must open, and before a channel can close or inactivate, it must first lose its ligand. This is expressed in the following simple-state diagram for the sodium channel. R_0–R_2, O, and I refer to resting-closed, open, and inactivated states, respectively; drug-occupied states are indicated by an asterisk. Only state O is conducting. The transition from R_0 to O can be described by Hodgkin and Huxley m^3-kinetics (scheme 1; Hodgkin and Huxley, 1952);

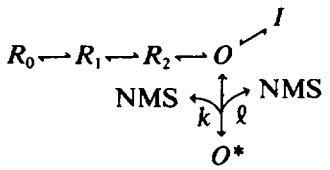

SCHEME 1

where k and ℓ are, respectively, binding and departure rates of NMS molecules. This model is similar to one proposed by Yeh and Narahashi (1977) for the action of pancuronium, another cationic sodium channel blocker effective internally. It is the simplest model that will explain the results of Figs. 1 and 2 and may serve as a frame of reference.

Block of Gating Current by NMS

From Armstrong and Bezanilla's hypothesis one might expect that if NMS blocks by insertion into the aqueous pore, it may immobilize the gating mechanism and cause block of gating current. Moreover, insofar as NMS blocks preferentially open channels, it should preferentially block "off"-gating current. This is most easily tested in pronase-treated axon, where normal inactivation can be almost completely removed (Fig. 3 A). In such axons, internal addition of NMS reintroduces a decline of sodium current resembling normal inactivation (Cahalan, 1978; not shown here). In Fig. 3 B and C gating currents were recorded after 0.5 μM external tetrodotoxin was added. As in Armstrong and Bezanilla's (1977) work, the pronase treatment removed normal charge immobilization along with inactivation, so on- and

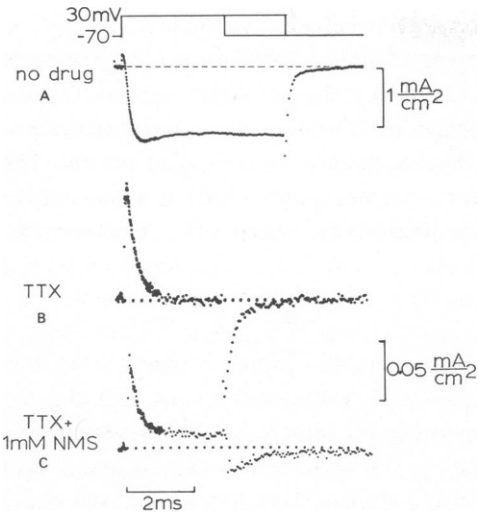

FIGURE 3

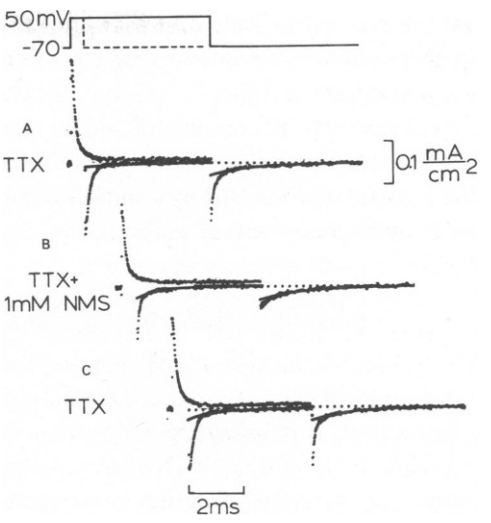

FIGURE 4

FIGURE 3 Sodium current (A) and gating current (B and C) during a pulse from −70 to +30 mV. Pronase-treated axon. Tetrodotoxin (TTX; 0.5 μM) applied as indicated. Trace B: on-charge, 18.5 nC/cm², off-charge 17.4 nC/cm². Trace C: on-charge 10.1 nC/cm², off-charge 7.1 nC/cm². These values were obtained by integrating over the first 1.6 ms (on) or 2.7 ms (off) following the potential change; horizontal base lines fit to the 1.3 ms after the integration interval were subtracted before integrating. Axon 86, Tris-ASW//200 Cs, 8°C.

FIGURE 4 Superimposed records of gating currents during and after pulses of 0.5- and 5-ms duration. NMS applied as indicated. Solid lines are declining exponentials fitted to segments of traces starting 0.69 – 0.89 ms after repolarization and ending 0.5 – 1.5 ms later. Time constants and amplitudes of exponentials for 5-ms pulses were: 12.5 μA/cm² and 1.47 ms (A); 13.4 μA/cm² and 1.63 ms (B), 12.7 μA/cm² and 1.59 ms (C). On-charge during 5-ms pulses was 19.3 nC/cm² (A), 15.3 nC/cm² (B) and 19.2 nC/cm² (C). They were obtained by integrating over the first 1.7 ms of depolarization after subtracting horizontal base lines fitted to the following 2 ms. Tris-ASW//200 Cs, 8°C. Same axon as in Fig. 1.

rapid off-transients carried nearly equal charge. After adding NMS, the on-transient of asymmetry current is reduced and a steady outward component appears during the pulse. Both changes are probably due to accelerated deterioration which often follows pronase treatment. A steady outward component in particular is expected if leakage conductance is increased and not perfectly ohmic. Most importantly, however, the rapid off-charge movement seen before adding NMS is now greatly reduced. This is qualitatively consistent with the idea that NMS both blocked and immobilized the sodium channel, possibly assuming a role normally served by an endogenous "inactivating particle" which in this experiment was lost during pronase treatment.

If upon repolarization NMS escaped from sodium channels as rapidly in the experiment of Fig. 3 as it did in that of Fig. 2, then one may expect to see in Fig. 3 C an off-transient that (*a*) carries the same charge as the on-transient and (*b*) has a time-course similar to that of the sodium current tails in Fig. 2 (left). *b* is expected if drug unbinding ($O^* \rightarrow O$) and channel closing ($O \rightarrow R_2$) together take more time than, and are thus rate-limiting for, all subsequent transitions producing off-gating current. However, tetrodotoxin was used here and may have retarded escape of NMS after repolarization to an unknown extent. Such an effect of

tetrodotoxin would be in line with the observed synergism between the toxin and QX-314, another cationic internal blocking particle (Cahalan and Almers, 1979*a*). Fig. 3 C does show an off-transient carrying 7.2 nC/cm^2 as compared to the 10.1 nC/cm^2 under the on-transient. However, slow off-transients of similar size and shape are often seen also in the absence of NMS and we are not sure how much of the slow off-transients is sodium gating current. The off-transient can be fitted by a single exponential of τ = 1.5 ms, roughly 3–5 times slower than the final time constants of sodium current tails in the presence of NMS (0.33 ± 0.06 ms, 8°C, n = 3).

Time-Course of Gating Current Block

NMS-induced block of off-gating current was seen also in axons with intact inactivation. Fig. 4 shows gating currents recorded from the axon of Figs. 1–2. Traces with a short (0.5 ms) and a long (5 ms) depolarizing pulse to 50 mV are superimposed. Whereas the on-transient was only slightly diminished by NMS, the drug blocked the fast off-transient rapidly and almost completely. A slow off-transient remained both with and without the drug; it is not considered further. The rapid off-transients recovered partially after drug withdrawal (Fig. 4 C). For a quantitative analysis of this experiment, declining exponentials were fitted to the later portions of the off-transients (solid lines in Fig. 4) and subtracted from the record. The time integral of the remaining rapid off-transient (Q_{off}) was divided by the on-charge (Q_{on}) and plotted against pulse duration in Fig. 6 A. NMS is seen to speed the decline of Q_{off}/Q_{on}, just as it speeded the decline of sodium inward current in Fig. 1. The curves were derived from sodium current measurements on the same axon as described later; they fit the data well.

Fig. 5 shows an experiment similar to that of Fig. 4, but at a higher temperature. Again, NMS reversibly causes rapid block of off-gating current. Analysis of the experiment as described above gave the results in Fig. 6 B. Once more, NMS speeds the decline of Q_{off}/Q_{on}. The experiment of Figs. 4 and 5 was tried on five other axons at 8 or 16°C. NMS always hastened charge immobilization, even though not always as dramatically as in Fig. 4.

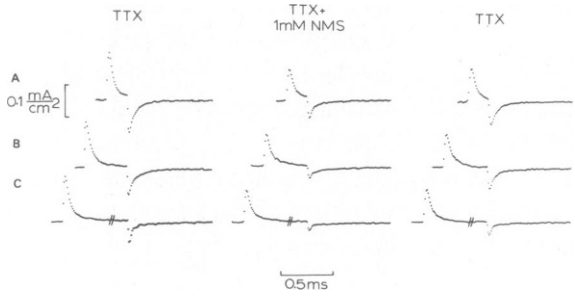

FIGURE 5 Gating currents during and after pulses from −70 to +50 mV of duration 0.2 ms (A), 0.5 (B), and 4.0 ms (C). In row C, on-charges were 23.4 nC/cm^2 (TTX), 21.3 nC/cm^2 (TTX + 1mM NMS), and 22.6 nC/cm^2 (TTX). They were obtained by integrating over the first 0.89 ms of the pulse, after subtracting a horizontal base line fitted to the following 0.68 ms. Slashes indicate where a section of the trace was removed to save space. NMS (1 mM) present as indicated. For later analysis (Fig. 14), single exponentials (not shown) were fitted to 0.6-ms-long segments starting 0.38 ms after repolarization. For the bottom row, their amplitudes and time constants were: 27 μA/cm^2 and 0.76 ms (TTX), 17.2 μA/cm^2 and 0.87 ms (TTX + 1 mM NMS) and 44 μA/cm^2 and 1.19 ms (TTX). Tris-ASW//200 Cs. 16°C, axon 200.

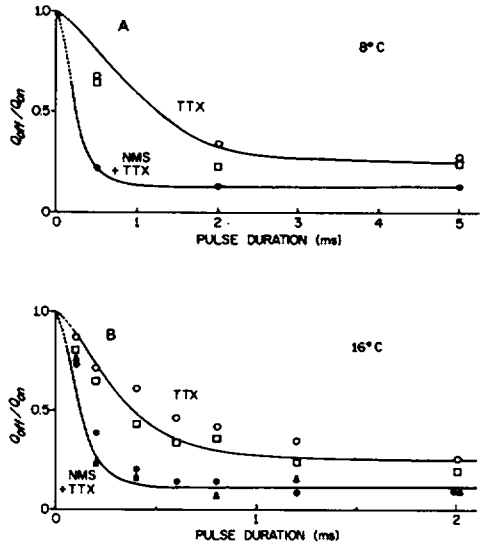

FIGURE 6 Analysis of experiments in Figs. 4 and 5 and comparison with sodium current data of Fig. 7. Q_{on} was measured after subtracting horizontal base lines during 4-5 ms pulses and then integrating over the pulse duration. Q_{off} was measured after subtracting single exponentials as in Figs. 4 and 5. Measurements made before (○), during (●, ▲), and after (□) presence of 1 mM internal NMS. A: Axon 81, same as in Figs. 1, 4, and 7. Solid curves were based on a model (Eq. 5) where inactivation was coupled in series to a Hodgkin-Huxley activation process. In Fig. 7C, let $f(t)$ be the curve without and $g(t)$ the curve with NMS. Then the solid curves $F(t)$ and $G(t)$ in Fig. 6A were obtained from $f(t)$ and $g(t)$ by scaling and adding a constant as follows: $F(t) = 0.88\, f(t) + 0.12$ (no drug) and $G(t) = 0.9\, g(t) + 0.1$ (NMS present). B: Data points from axon 200 (Fig. 5), curves from Fig. 7D. Significance of curves and nomenclature as in A. $F(t) = 0.79\, f(t) + 0.21$ (no drug) and $G(t) = 0.91\, g(t) + 0.09$ (NMS present).

A slight decrease of on-gating current, as seen in Figs. 4 and 5, was consistently observed when NMS was added to tetrodotoxin-poisoned fibers, and when rapidly repeating pulses were used for signal averaging. The effect resembles that of QX-314 (Cahalan and Almers, 1979*a*) but is smaller. As with QX-314, an accumulating block under repetitive depolarization (Cahalan, 1978) and a slow recovery from it' are seen also with NMS. We have not investigated this NMS-induced block of on-gating current, but it may arise in the same way as with QX-314 and other local anesthetics.

Comparison of Sodium and Gating Current Block

So far, our findings are qualitatively consistent with scheme 1 and Armstrong and Bezanilla's hypothesis. Resting, nonconducting channels are largely drug free, and depolarization opens them in a normal fashion, eliciting essentially normal on-gating current. NMS then enters the channel, blocking ion flow. Upon repolarization, channels cannot close as long as NMS remains stuck in them, and the usual rapid off-gating current is absent. As a further test of this hypothesis, we now compare quantitatively the time-course of sodium and gating current block.

Because no mathematical model has yet been proposed that describes both sodium conductance changes and gating currents, our quantitative treatment is necessarily empirical and approximate. We follow scheme 1 which contains the following implicit assumptions. (*a*)

A blocked channel passes no current, and an unblocked channel is normal in all respects. Thus all sodium current is due to normal channels, and the complex kinetic effects in Figs. 1 and 2 are all due to drug-channel interactions that depend on voltage and on whether the channel is open. (*b*) We neglect certain subtle features of sodium channel gating that led Armstrong and Bezanilla (1977) to postulate two open states, and Chiu (1977) to assume two inactivated states. Thus we make no distinction between Armstrong and Bezanilla's open states x_1 and x_1y and none between Chiu's inactivated states 1 and 2. Also we do not consider at this stage a third open state, h_2, postulated by Chandler and Meves (1970). With regard to gating current, we further assume that except for an immobilization-resistant fraction β (or β^* in NMS), Q_{off} will contain contributions only from sodium channels that are neither blocked nor inactivated. Then for sufficiently long pulses, we have

$$\frac{Q_{off}}{Q_{on}} = (1 - \beta)\frac{O}{O + I} + \beta$$

without drug, and in the presence of NMS

$$\frac{Q_{off}}{Q_{on}} = (1 - \beta^*)\frac{O}{O + O^* + I} + \beta^*,$$

where O is the occupancy of state O, I that of state I and so on. For extremely short pulses (<0.5 ms in Fig. 4 and <0.2 ms in Fig. 5), or for pulses to negative potentials, these equalities may fail if intermediate states in the sequence $R_0 \rightarrow \ldots \rightarrow O$ remain significantly populated.

The next aim is to derive the ratios $[O:(O + I)]$ and $[O:(O + O^* + I)]$ from the experiment of Fig. 1, which employed pulses to the same potential as those in Figs. 4 and 5. O is simply proportional to the Na^+ current at any moment in time; $(O + I)$ or $(O + O^* + I)$ is the sum of all channels that opened during depolarization. We would expect to record a Na^+ current proportional to these sums if states O^* and I were inaccessible as, e.g., in the absence of drug after pronase treatment. Therefore, the next step was to reconstruct the time-course of sodium channel opening ($R_0 \rightleftharpoons \ldots \rightleftharpoons 0$ in scheme 1) by kinetic modeling. For the experiment of Fig. 1 this resulted in the curves labeled "$\tilde{I}_{Na}m^3$" in Fig. 7 A and B. As described below $\tilde{I}_{Na}$ denotes the current with all channels open, and $m^3(t)$ the growth of current from zero to $\tilde{I}_{Na}$. The curves $\tilde{I}_{Na}m^3$ may be taken as the current that would have resulted in Fig. 1 had the transitions $O \rightarrow I$ and $O \rightarrow O^*$ been prevented, as, e.g., after pronase treatment in the absence of drug. These curves will be taken as a reference to which the measured currents in Fig. 1 can be compared. First, however, it is necessary to describe the modeling process.

In modeling sodium conductance changes, we follow Hodgkin and Huxley in describing the reaction $R_0 \rightleftharpoons \ldots \rightleftharpoons O$ by a first-order variable, m, raised to the third power. Although this formalism may not give a correct molecular description of sodium channel transitions, we consider it an accurate empirical description of the normal conductance change during depolarization (Hodgkin and Huxley, 1952), which is all that matters here. For inactivation one can consider two extreme models. In the first, inactivation is totally independent from activation and affects the R and O states identically (Hodgkin and Huxley, 1952):

$$I_{Na} = \tilde{I}_{Na}[1 - \exp(-t/\tau_m)]^3 \exp(-t/\tau_h), \qquad (1)$$

where $\tilde{I}_{Na}$ is the maximal sodium current I_{Na} with all channels open, and τ_m and τ_h are the

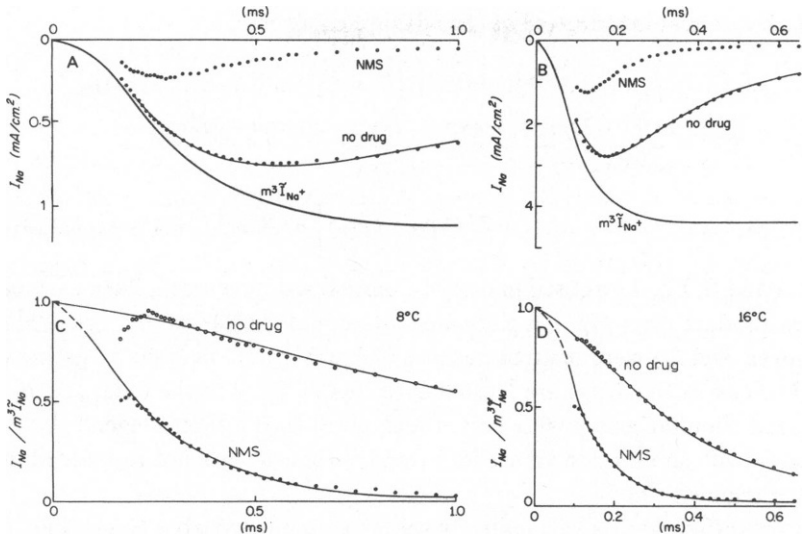

FIGURE 7 Analysis of the experiment in Fig. 1. A and B show the early portions of the traces in Fig. 1, replotted on an expanded time scale. The first 200 (A) or 100 μs (B) were omitted because of probable contamination by gating current. Curves labeled "no drug" are least-squares fits of Eq. 5 to the corresponding traces in Fig. 1; only the early portions are shown. Best parameters were: $\bar{I}_{Na} = 1.12$ mA/cm^2, $\tau_m = 0.17$ ms, $\tau_h = 0.87$ ms, $\beta = 0.13$ (A) and $\bar{I}_{Na} = 4.41$ mA/cm^2, $\tau_m = 0.060$ ms, $\tau_h = 0.25$ ms and $\beta = 0.059$ in B. Also shown are plots of $I_{Na} = m^3 \bar{I}_{Na}$, where $m = [1 - \exp(-t/\tau_m)]$, with τ_m as above. C and D show membrane currents with and without NMS divided by $m^3 \bar{I}_{Na}$. Curves labeled "no drug" are the right-hand side of Eq. 5 divided by $m^3 \bar{I}_{Na}$, with parameters as above. Curves labeled "NMS" are plots of $A \exp(-t/\tau_{NMS}) + B$, with $A = 1.7$; $\tau_{NMS} = 222$ μs and $B = 0$ (A and C) and $A = 1.7$; $\tau_{NMS} = 90$ μs and B = 0.025 (B and D).

reciprocal rate constants for m and h, the first-order variables for activation and inactivation. In a second model, inactivation is totally coupled to activation, as has been suggested by many authors, most recently by Armstrong and Bezanilla (1977), on the basis of gating current measurements. If the reaction $O \rightleftharpoons I$ proceeds with reciprocal rate τ_h, and the m^3 formalism is retained, it can be shown for scheme 1 that

$$I_{Na} = 3\bar{I}_{Na}\left\{\frac{2\exp(-2t/\tau_m)}{2 - \tau_m/\tau_h} - \frac{\exp(-t/\tau_m)}{1 - \tau_m/\tau_h} - \frac{\exp(-3t/\tau_m)}{3 - \tau_m/\tau_h} + C\exp(-t/\tau_h)\right\}, \quad (2)$$

where

$$C = \frac{1}{3 - \tau_m/\tau_h} - \frac{2}{2 - \tau_m/\tau_h} + \frac{1}{1 - \tau_m/\tau_h}.$$

Eq. 2 is derived in an appendix. In Eqs. 1 and 2, all channels are assumed to be in the resting state at $t = 0$ (i.e., $m = 0$ and $h = 1$) and in the inactivated state at $t \to \infty$ ($m = 1$ and $h = 0$), in other words, the reactions $R_0 \rightarrow\rightarrow O \rightarrow I$ are approximated as being irreversible. This seems reasonable during a strong depolarization from -70 mV. To include a small fraction of

channels, B, that cannot inactivate, Eqs. 1 and 2 are expanded:

$$I_{Na} = \tilde{I}_{Na}[1 - \exp(-t/\tau_m)]^3[B + (1 - B)\exp(-t/\tau_h)] \quad (3)$$

$$I_{Na} = 3\tilde{I}_{Na}(1 - B)\left[\frac{2\exp(-2t/\tau_m)}{2 - \tau_m/\tau_h} - \frac{\exp(-t/\tau_m)}{1 - \tau_m/\tau_h} - \frac{\exp(-3t/\tau_m)}{3 - \tau_m/\tau_h} + C\exp(-t/\tau_h)\right] + B\tilde{I}_{Na}[1 - \exp(-t/\tau_m)]^3. \quad (4)$$

In Fig. 7 A and B, Eq. 4 was used to describe normal sodium current during depolarization. Filled circles are data from Fig. 1 replotted on an expanded abscissa; the first 200 μs (A and C) or 100 μs (B and D) were omitted because of heavy contamination by gating current at that time. The curves (no drug) are least-squares fits of Eq. 4 to the data; $\tilde{I}_{Na}$, B, τ_m and τ_h were optimized simultaneously with best values given in the figure legend. Eq. 3 gave an equally good fit with similar best values for τ_m and τ_h (not shown), but $\tilde{I}_{Na}$ needed to be larger and B smaller than with Eq. 4.

Now the activation process is completely specified by the variable $\tilde{I}_{Na}m^3$. Fig. 7 C and D show currents with and without NMS divided by $\tilde{I}_{Na}m^3$. Curves labeled "no drug" thus plot the ratio O:$(O + I)$ as a function of time, and trace out the time-courses of inactivation in Fig. 1. Under our assumptions, the filled circles plot the ratio O:$(O + O^* + I)$. After 200 (A and C) or 150 μs (B and D), the points are approximated reasonably well by single exponentials. At earlier times, a single exponential fails; this is at least partly due to contamination by gating current and would also be expected if inactivation and block cannot occur before channel opening.

Sodium and gating current experiments can now be compared. The curves in Fig. 6 are the same as in Fig. 7 C and D except for scaling and adding a constant to allow for immobilization-resistant off-charge movement. The data in Fig. 6 A and Fig. 7 C in particular were derived from the same axon. There are minor discrepancies between data points and curves in Fig. 6 which may be due to measurement uncertainties. On the whole, however, we consider the agreement between sodium and gating current data satisfactory. Our experiments confirm the more extensive observations of Armstrong and Bezanilla (1977) that sodium current inactivation and charge immobilization in normal axons happen simultaneously. Most importantly, however, they also show that NMS effects on sodium conductance and off-gating current follow closely similar time-courses, and are therefore probably linked. When NMS moves into and blocks open sodium channels, it evidently also immobilizes gating charge. We may therefore have found an artificial substitute for the physiological inactivating particle postulated by Armstrong and Bezanilla (1977).

Rate Constants for Block and Unblock

BLOCK DURING DEPOLARIZATION After 150–200 μs, the decline of the ratio [O:$(O + O^* + I)$] in Fig. 7 is reasonably well fitted by single exponentials with time constants, τ_{NMS}, of 220 (C) and 90 μs (D). For scheme 1 one expects in general two phases of decline, a rapid one due to reactions

$$O \xrightarrow{k} O^*$$

and

$$O \xrightarrow{1/\tau_h} I,$$

as well as a slower one due to reaction

$$O^* \xrightarrow{\ell} O \xrightarrow{1/\tau_h} I,$$

where τ_h is the reciprocal rate of inactivation in the model of Eq. 4. Slow and fast phases of decline are sometimes seen,[1] but in Fig. 7 the rapid phase apparently predominated and brought virtually complete (>97%) decline of the ratio $[O:(O + O^* + I)]$. This suggests that in Fig. 7, $\ell << (a + k)$, in which case

$$\frac{1}{\tau_{NMS}} = k + \frac{1}{\tau_h}.$$

With τ_h = 0.87 (A and C) and 0.25 ms (B and D), the rate k becomes 4.0/ms (A and C) and 7.1/ms (B and D).

If the $m^3\tilde{I}_{Na}$ trace is obtained by using the orthodox Hodgkin-Huxley model, the ratio $I_{NMS}:m^3\tilde{I}_{Na}$ can also be fitted by single exponentials with τ_{NMS} = 185 μs (C) and τ_{NMS} = 90 μs (D). As in Fig. 7, exponentials extrapolate to values greater than unity for t = 0, as expected if NMS cannot block the resting channel. The Hodgkin-Huxley description of inactivation is now well known to be inconsistent with gating current properties and will be abandoned at this stage in favor of scheme 1 and Eq. 4.

Another way to demonstrate that the interaction between channel and drug is time dependent is to measure the final time constant of sodium tails and plot them against pulse duration. Fig. 8 shows data from the axon of Fig. 2 (right). Without drug, final time constants do not change strongly with pulse duration, whereas in the presence of NMS, there is a pronounced increase which probably reflects the time-dependent entry of the drug into sodium channels. An exponential fitted to the early points extrapolates to τ = 40 μs, suggesting that

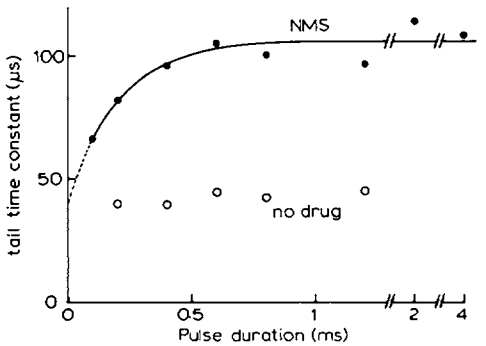

FIGURE 8 Final time constant (ordinate) of sodium current tail after pulses to 50 mV of varying duration (abscissa). Same experiment as in Fig. 2 (right), where original records of some of the tails are shown. the NMS curve is an exponential with time constant 0.19 ms; its value at t = 0 is 40 μs. Axon 198, 16°C.

after pulses too brief to permit NMS entry, the rate of sodium channel closing is close to normal.

UNBLOCK AFTER REPOLARIZATION The large inward current tails accompanying repolarization in Fig. 2 indicate that repolarization clears NMS out of sodium channels. In a quantitative analysis of these tails we consider only states R_2, O, and O^* since states R_1, R_0, and I contribute no current and the rate constants associated with I (i.e, for recovery from inactivation) are too slow to matter. Assume that at the end of a depolarizing pulse, all noninactivated channels are blocked but open (O^*), and that upon repolarization, they all ultimately lose their ligand and close; further assume that reactions $R_0 \longrightarrow \longrightarrow O$ are negligible at -70 mV. In Hodgkin-Huxley nomenclature, this would correspond to assuming that the parameter m declined from unity to zero upon repolarization:

$$O^* \underset{k}{\overset{\ell}{\rightleftharpoons}} O \underset{a}{\longrightarrow} R_2 \longrightarrow R_1 \longrightarrow R_0.$$

With these assumptions, the fraction of open channels, O, can be shown to be

$$O = C[\exp(-t/\tau_s) - \exp(-t/\tau_f)], \tag{5}$$

where C is a constant and the slow and fast time constants, τ_s and τ_f, are

$$1/\tau_f = \tfrac{1}{2}(a + k + \ell + \sqrt{(a + k + \ell)^2 - 4a\ell})$$
$$1/\tau_s = \tfrac{1}{2}(a + k + \ell - \sqrt{(a + k + \ell)^2 - 4a\ell}). \tag{6}$$

Because $dO/dt = \ell O_0^*$ for $t = 0$, we have

$$C = O_0^* \frac{1}{\sqrt{(a + k + \ell)^2 - 4a\ell}},$$

where O_0^* is the occupancy of O^* at the instant of repolarization. The time integral of Eq. 5 is

$$\int_0^\infty O(t)\, dt = \frac{O_0^*}{a}, \tag{7}$$

a result that will be used in a later paper.

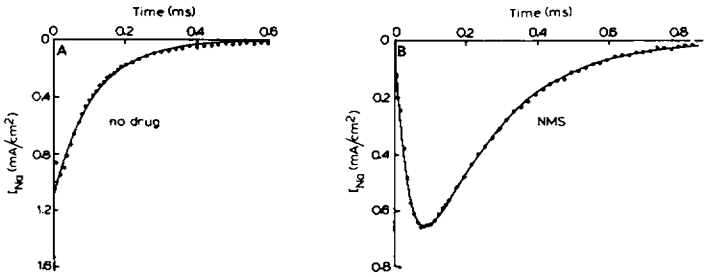

FIGURE 9 Analysis of tail currents after a 2-ms depolarization to +50 mV. Data (•) were taken from Fig. 2 (axon 81) and replotted on an expanded abscissa. Curves are given by $I_{Na} = C \exp(-3t/\tau_m)$ (A) and by Eq. 6 (B, 1 mM NMS). In the solid curves, the parameters C, τ_m, τ_s, and τ_f were adjusted to give the best least-squares fit to the data. Their values were $C = 1.11$ mA/cm², $\tau_m/3 = 113$ μs (no drug), and $C = 1.29$ mA/cm², $\tau_s = 205$ μs, $\tau_f = 45.3$ μs (NMS).

Fig. 9 shows tail currents at −70 mV after a 2-ms pulse to +50 mV with (B) and without (A) NMS; they were taken from Fig. 2 (left) and replotted on an expanded abscissa. The solid lines are least-squares fits of a single exponential (A) and Eq. 5 (B). (With the reasonable assumption that m changed from one to zero in Fig. 9, a single exponential with time constant $\tau_m/3$ would be predicted by the Hodgkin-Huxley model for the normal closing of sodium channels at −70 mV.) In Fig. 9 A, the best value was $\tau_m/3 = 113$ μs. In the presence of NMS, the time constants giving the best least-squares fit of Eq. 5 to the data were $\tau_f = 43.3$ μs and $\tau_s = 205$ μs, twice faster and twice slower than $\tau_m/3$. Similar results obtained on three other axons are summarized in Table I. The last two columns in Table I were calculated by letting $a = 3/\tau_m$ as demanded by scheme 1. In that case one obtains from Eqs. 5 and 6

$$\ell = \frac{\tau_m}{3\,\tau_f \tau_s}$$

$$k + \ell = \frac{1}{\tau_f} + \frac{1}{\tau_s} - \frac{3}{\tau_m}.$$

At −70 mV, the "relaxation time constant" $1/(k + \ell)$ of the reaction $O^* \rightleftharpoons O$ would then be similar to (or smaller than) the time constant for normal channel closing. The mean products of the last two columns $\ell/(k + \ell)$, are 0.50 (axon 80), 0.69 (axon 81), 0.70 (axon 198), and 0.55 (axon 199). These values would give the equilibrium fraction of open channels at −70 mV which would become drug free and conducting. In other words, if the reaction $O^* \rightleftharpoons O$ had time to reach equilibrium at −70 mV, approximately one-half to one-third of all open

TABLE I
KINETICS OF TAIL CURRENTS FOLLOWING REPOLARIZATION

		No drug			1 mM NMS				
Axon		Pulse duration	$[Na]_o$	$\tau_m/3$	$[Na]_o$	τ_S	τ_f	ℓ	$1/(k+\ell)$
No.	°C	*ms*	*M*	*μs*	*M*	*μs*	*μs*	*μs*$^{-1}$	*μs*
80	8	2	0.44	90	0.44	368	44.7	0.0055	71.5
		4		168		346	65.9	0.0074	82.6
		8				333	60.4	—	—
81	8	0.5	0.44	100	0.44	162	33.7	0.0183	38.7
		2		113		205	45.3	0.0122	55.2
		5		129		227	48.3	0.0118	57.6
198	16	0.2	0.11	39.5	0.44	—	—		
		0.4		39.5		90.2	25.5	0.0172	40.0
		0.6		44.3		103	28.0	0.0154	43.8
		0.8		42.5		95.9	29.4	0.0151	47.8
		1.2		44.8		92.6	28.5	0.0170	42.4
		2		—		101	31.3	—	—
		4		—		107	29.9	—	—
199	16	0.2	0.11	52.4	0.44	—	—	—	—
		0.4		51.2		108	17.9	0.0265	21.9
		0.6		48.1		125	22.0	0.0175	30.6
		0.8		49.6		135	22.9	0.0160	32.3
		1.2		54.0		131	23.6	0.0175	31.8
		2		—		122	22.5	—	—
		4		—		118	20.7	—	—

channels would remain blocked. As it happens, state O is unstable at -70 mV so all channels eventually return to the resting state and lose their ligand.

DISCUSSION

In this paper, we attempt a quantitative analysis of some strychnine effects in axons with intact inactivation. Our findings are analyzed in the context of a model in which strychnine can bind to only the open channel, and in which unblocked channels are normal. On this basis, we conclude that at an internal potential of 50 mV, 1 mM internal NMS blocks virtually all open channels with time constants of the order of 100 (16°C) or 200 μs (8°C). Repolarization to -70 mV pulls NMS back into the axoplasm; if channels at -70 mV remained open indefinitely, this would proceed with time constants of $\simeq$ 40 (16°C) or 60 μs (8°C) until $\frac{1}{2}$–$\frac{2}{3}$ of all channels have become unblocked. The model of scheme 1 may be unduly simple and will ultimately need expansion;[1] thus our analysis of rate constants, particularly that in Table I, must be regarded as tentative. Nevertheless some basic features of the model seem well substantiated. In particular it appears that NMS molecules can bind (and remain bound) to open channels only. Thus, as seen in Fig. 1, traces with and without drug superimpose closely during the first 100–200 μs. This indicates that block occurs only after a delay, as expected if the channel must open before it can be blocked. Furthermore, closing of channels upon repolarization is slowed (tails in Fig. 2) as expected if channels can close only after NMS has unbound. The characteristic time-course of tails in particular can be quantitatively accounted for on that basis. Finally, block of virtually the entire rapid off-gating current by NMS is another indication that as long as the drug is present in the channel, the voltage-dependent conformational changes necessary for channel closing are prevented. Other features of block by NMS are discussed elsewhere (Cahalan, 1978).[1] In particular, we have not discussed here the "use-dependent block" by NMS, an effect that develops under repetitive stimulation, recovers over a time scale of several seconds (Cahalan, 1978) and resembles that of QX-314. Interference from this component of block in sodium current experiments was minimized by allowing a 20–30-s rest period before each depolarization. In gating current experiments, use-dependent block by NMS may have caused the small decrease of on-gating current; this happens also in the presence of QX-314 (Cahalan and Almers, 1979*a*).

The main finding of this paper is that block of sodium current by NMS is accompanied by charge immobilization. There is good temporal correlation between block of gating and sodium current during depolarization, but not after repolarization. In particular, an expected gating current transient with the time-course of sodium tails in, e.g., Fig. 2, is absent in Figs. 3, 4, and 5, as if recovery of gating charge from immobilization in NMS-poisoned axons were slower than the rate of drug escape inferred from sodium current measurements. However, measurements of off-gating current are necessarily made in presence of tetrodotoxin or saxitoxin, and there is now clear evidence that tetrodotoxin can affect the interaction between channel and an internal cationic blocking particle (Cahalan and Almers, 1979*a*). We feel that the other kinetic parallels between sodium and gating current block, which we did observe, leave little doubt that both effects are linked.

There are several parallels between block by NMS and physiological inactivation. Both inactivation (Bezanilla and Armstrong, 1977) and block by NMS occur after a delay, as if they could operate only on open channels. Both effects are accompanied by charge immobili-

zation. Furthermore, after abolition of inactivation by pronase treatment, NMS can reintroduce a decline of sodium current resembling inactivation as well as charge immobilization. Finally, NMS can protect against (or compete with) inactivation, as if a physiological inactivation particle and NMS competed for the same (or closely adjacent) sites. Given the strong possibility that NMS blocks by insertion into the aqueous pore, our findings fit well with Armstrong and Bezanilla's (1977) hypothesis for sodium channel inactivation. NMS may well act as an artificial substitute for an endogenous blocking particle responsible for inactivation.

Unlike inactivation, however, block by NMS is accompanied by virtually complete charge immobilization. Thus a lower limit on the "purity of gating currents" (Almers, 1978) can be moved upwards. In Fig. 6, at least 90% of the rapid charge movement is immobilized by NMS, and thus probably sodium channel gating current. The 10% charge remaining in Fig. 6 could well be due to drug-free, normally inactivated channels. Virtually complete charge immobilization by NMS confirms the view that the charge movement which remains after normal inactivation is related to voltage-dependent transitions of the inactivated channel (Armstrong and Benzanilla, 1977).

Recently, Yeh and Armstrong (1978) have made similar observations with the sodium channel blocker pancuronium. Now there are three well-studied cationic compounds causing charge immobilization as they block sodium channels: NMS, pancuronium, and QX-314. Each of them is effective only from the inside. A second group of cationic blockers—tetrodotoxin and saxitoxin—are effective only from the outside but cause little or no charge immobilization (Armstrong and Bezanilla, 1974; Keynes and Rojas, 1974) and show no detectable interaction with the gating mechanism (Almers and Levinson, 1975). These findings are well in line with the general view that the gating machinery of the sodium channel is comparatively more accessible from the axoplasmic side. With QX-314, it was not clear whether the drug caused immobilization directly, or indirectly by causing inactivation. The situation with NMS and pancuronium is clearer. Both must cause immobilization directly, because both compete with normal inactivation and cause block and immobilization also in pronase-treated axons.

It is a pleasure to thank Ms. Suzanne Marble for her help with typing and data analysis, Doctors Bertil Hille, Peter Detwiler, and Wolfgang Nonner for their comments on various drafts of the manuscript, and Dr. Clay M. Armstrong for providing laboratory space at the Marine Biological Laboratory, Woods Hole, Mass. We are indebted to Dr. Eberhard Fetz and Dr. Theodore Kehl (supported by U.S. Public Health Service grant RR-00374), both at the University of Washington, for the use of their computer facilities for data analysis. Dr. Cahalan was supported by a postdoctoral fellowship from Muscular Dystrophy Associations of America, Inc.

This work was supported by U.S. Public Health Service grants AM-17803 to Dr. Almers and NS-08951 to Dr. C. M. Armstrong.

Received for publication 5 July 1978 and in revised form 12 January 1979.

APPENDIX

Eq. 3 in the text is based on the following reaction sequence:

$$R_0 \underset{\beta_m}{\overset{3\alpha_m}{\rightleftharpoons}} R_1 \underset{2\beta_m}{\overset{2\alpha_m}{\rightleftharpoons}} R_2 \underset{3\beta_m}{\overset{\alpha_m}{\rightleftharpoons}} O \underset{\alpha_h}{\overset{\beta_h}{\rightleftharpoons}} I,$$

where, in the Hodgkin-Huxley model (1952), O and I are open and inactivated states and R_0, R_1, and R_2

resting states with zero, one, and two m-particles in the activating position. The rates β_m, α_h for the backward reactions are neglected here, because we wish to model the sodium channel during extreme depolarization only. For a depolarization starting at $t = 0$, and $R_0 = 1$ at $t = 0$,

$$R_0 = \exp(-3\alpha_m t) \tag{A1}$$

and

$$\frac{dR_1}{dt} = 3\alpha_m R_0 - 2\alpha_m R_1, \tag{A2}$$

where R_0 and R_1 are the fractional occupancies of states R_0 and R_1. Similarly, R_2 and O will denote the fractional occupancies of states R_2 and O. Eq. A2 is of the form

$$\frac{dy}{dt} = f(t) - ky,$$

with the general solution

$$y(t) = C\exp(-kt) + \exp(-kt)\int f(t)\exp(kt)\,dt. \tag{A3}$$

Thus in our case

$$R_1(t) = C_1\exp(-2\alpha_m t) - 3\exp(-3\alpha_m t)$$

and, for $R_1(t) = 0$ at $t = 0$,

$$R_1(t) = 3[\exp(-2\alpha_m t) - \exp(-3\alpha_m t)]. \tag{A4}$$

Continuing the sequence, one has for state R_2:

$$\frac{dR_2}{dt} = 2\alpha_m R_1 - \alpha_m R_2, \tag{A5}$$

which can be solved as above:

$$R_2(t) = 3[\exp(-\alpha_m t) - 2\exp(-2\alpha_m t) + \exp(-3\alpha_m t)]. \tag{A6}$$

Finally,

$$\frac{dO}{dt} = \alpha_m R_2 - \beta_h O, \tag{A7}$$

which can be solved as under Eq. A3:

$$O = 3\alpha_m\left[\frac{2\exp(-2\alpha_m t)}{2\alpha_m - \beta_h} - \frac{\exp(-\alpha_m t)}{\alpha_m - \beta_h} - \frac{\exp(-3\alpha_m t)}{3\alpha_m - \beta_h} + C\exp(-\beta_h t)\right]. \tag{A8}$$

Writing $\alpha_m = 1/\tau_m$ and $\beta_h = 1/\tau_h$, Eq. 8 becomes

$$O = 3\left[\frac{2\exp(-2t/\tau_m)}{2 - \tau_m/\tau_h} - \frac{\exp(-t/\tau_m)}{1 - \tau_m/\tau_h} - \frac{\exp(-3t/\tau_m)}{3 - \tau_m/\tau_h} + C\exp(-t/\tau_h)\right]. \tag{A9}$$

The integration constant C can be evaluated by setting O zero at zero time; it then assumes the value given in Eq. 3. Because $I_{Na} = \bar{I}_{Na}O$, Eq. 3 in the text follows.

When $\tau_h \rightarrow \infty$ as after pronase treatment,

$$O = 3\{\exp(-2t/\tau_m) - \exp(-t/\tau_m) - \tfrac{1}{3}\exp(-3t/\tau_m) + \tfrac{1}{3}\},$$

which can be rewritten

$$O = [1 - \exp(-t/\tau_m)]^3,$$

as in the Hodgkin-Huxley model.

REFERENCES

ALMERS, W. 1978. Gating currents and charge movements in excitable membranes. *Rev. Physiol. Biochem. Pharmacol.* **82**:96–190.

ALMERS, W., and S. R. LEVINSON. 1975. Tetrodotoxin binding to normal and depolarized frog muscle and the conductance of a single sodium channel. *J. Physiol. (Lond.).* **247**:483–509.

ARMSTRONG, C. M. 1969. Inactivation of the potassium conductance and related phenomena caused by quaternary ammonium ion injection in squid axons. *J. Gen. Physiol.* **54**:553.

ARMSTRONG, C. M. 1971. Interaction of tetraethylammonium ion derivatives with the potassium channels of giant axons. *J. Gen. Physiol.* **58**:413–437.

ARMSTRONG, C. M., and F. BEZANILLA. 1974. Charge movement associated with the opening and closing of the activation of the Na channels. *J. Gen. Physiol.* **63**:533–552.

ARMSTRONG, C. M., and F. BEZANILLA. 1977. Inactivation of the sodium channel, II. Gating current experiments. *J. Gen. Physiol.* **70**:567–590.

ARMSTRONG, C. M., F. BEZANILLA, and E. ROJAS. 1973. Destruction of sodium conductance inactivation in squid axons perfused with pronase. *J. Gen. Physiol.* **62**:375–391.

CAHALAN, M. D. 1978. Local anesthetic block of sodium channels in normal and pronase-treated squid giant axons. *Biophys. J.* **23**:285–311.

CAHALAN, M. D., and W. ALMERS. 1979*a*. Interaction between quaternary lidocaine, the sodium channel gates, and tetrodotoxin. *Biophys. J.* **27**:39–56.

CAHALAN, M. D., and B. SHAPIRO. 1976. Current and frequency dependent block of sodium channels by strychnine. *Biophys. J.* **16**:76*a*. (Abstr).

CHANDLER, W. K., and H. MEVES. 1970. Evidence for two types of sodium conductance in axons perfused with sodium fluoride solution. *J. Physiol. (Lond.).* **211**:653–678.

CHIU, S. Y. 1977. Inactivation of sodium channels: second order kinetics in myelinated nerve. *J. Physiol. (Lond.).* **273**:573–596.

HILLE, B. 1977*a*. The pH-dependent rate of local anesthetics on the node of Ranvier. *J. Gen. Physiol.* **69**:475–496.

HILLE, B. 1977*b*. Local anesthetics: hydrophilic and hydrophobic pathways for the drug-receptor reaction. *J. Gen. Physiol.* **69**:497–515.

HODGKIN, A. L., and A. F. HUXLEY. 1952. A quantitative description of membrane current and its application to conduction and excitation in nerve. *J. Physiol. (Lond.).* **117**:500–544.

KEYNES, R. D., and E. ROJAS. 1974. Kinetics and steady state properties of the charged system controlling sodium conductance in the squid giant axon. *J. Physiol. (Lond.).* **239**:393–434.

SHAPIRO, B. I. 1977*a*. Effects of strychnine on the sodium conductance of the frog node of Ranvier. *J. Gen. Physiol.* **69**:915–926.

SHAPIRO, B. I. 1977*b*. Effects of strychnine on the potassium conductance of the frog node of Ranvier. *J. Gen. Physiol.* **69**:897–914.

YEH, J. Z., and C. M. ARMSTRONG. 1978. Immobilization of gating charge by a substance that simulates inactivation. *Nature (Lond.).* **273**:387–389.

YEH, J. Z., and T. NARAHASHI. 1977. Kinetic analysis of pancuronium interaction with sodium channels in squid axon membranes. *J. Gen. Physiol.* **69**:293–323.